Analysis of the pulse signal propagation in a turn of a meander line of two segments based on lattice diagrams

Analysis of the pulse signal propagation in a turn of a meander line of two segments based on lattice diagrams

P V Mikola, Z M Kenzhegulova and R S Surovtsev

Tomsk State University of Control Systems and Radioelectronics, 40, Lenin Ave., Tomsk, 634050, Russia

E-mail: mikolapavell@gmail.com

Abstract. The analysis of the propagation of a pulse signal in a turn of a meander line of two segments is carried out. For this purpose, the plotting of lattice diagrams for the even and odd modes is carried out, as well as their subsequent comparison with the time responses to the pulse excitation in each node of the line. A complete coincidence of the amplitudes and arrival times of pulses obtained by different methods was obtained.

1. Introduction

An important stage in the design of radio-electronic equipment (REE) is to ensure the requirements for their electromagnetic compatibility (EMC). One of the EMC aspects is to ensure the REE noise immunity of critical objects [1]. Because the packaging of PCBs is becoming increasingly dense, the operating voltages of internal elements are decreasing, and the frequency range of useful signals is increasing, the REE is becoming more and more sensitive to electromagnetic excitations [2, 3].

During the exploitation of critical REE (for example, communication systems), the danger is the intentional use of generators of powerful ultrashort pulses (USPs) to destabilize the operation of the object [4]. The specificity of the USP excitation is that its interference can be perceived as useful signals, however, disrupting the digital exchange. Meanwhile at higher amplitudes, they penetrate through traditional protection means and lead to REE failure [5], even over power circuits [6]. Traditional devices are not always able to provide protection against USPs because of a number of disadvantages (dielectric breakdown at high voltages, parasitic parameters, low speed) [7]. Therefore, it is necessary to search for new approaches to ensure REE protection against USPs and to improve the known protection means.

One of the principles of protection against USPs is their decomposition into a sequence of pulses of lower (relative to the original) amplitudes in meander lines of a special configuration [8]. Traditionally, meander lines are used to delay a signal on a PCB when it is clocked at the receiving point. Therefore, a significant part of the study of meander lines is aimed at analyzing signal distortions in such structures [9, 10]. At the heart of the protection devices is the phenomenon of modal decomposition of the interference signal (decomposition into components due to the difference in their propagation speeds) [11]. Thus, using numerical simulation, the USP decomposition in a meander line turn with an irregular cross-section has been studied, and the first analysis results for a

meander turn consisting of two segments with different cross-section parameters are presented [12]. As a result, additional pulses at the line end were identified, which arise because of the mismatch at the junction of the segments. Cross-section optimization that increases the amplitudes of these pulses can be a resource for additional attenuation of the USP. Since the results of the analysis were obtained using numerical simulation, then for a more complete understanding of the causes of signal distortions, it is advisable to evaluate it analytically. Such estimates are easy to obtain on the basis of lattice diagrams [13]. Meanwhile, a turn of a meander line is a rather complex structure. Therefore, first, we analyze a simpler structure (a one-conductor transmission line of two segments) using lattice diagrams, but taking into account the termination of the second segment represented as open circuit (OC) and short circuit (SC) [14]. This choice of terminations is caused by the fact that the intersection between the conductors at the end of the meander is characterized by an OC for an even mode and an SC for an odd one. The aim of this paper is to analyze the propagation of a pulse signal in a turn of a meander line using lattice diagrams.

2. Initial data for simulation

For investigation, a turn of a meander microstrip line of two segments was chosen. The cross-section view of each segment of the turn corresponds to a pair of coupled lines (Figure 1a) with the following parameters: the widths of the conductor of the first ($w1$) and second (w_2) segments are 400 and 200 μm, respectively; the foil thickness (t) is 35 μm; the distance between the conductors of the first and second segments (s) is 100 μm; the thickness of the substrate (h) is 510 μm; the relative permittivity of the substrate (ε_r) *is* 10; the distance from the edge of the structure to the conductor (d) is 3w. Figure 1*b* shows the circuit diagram of the line under investigation.

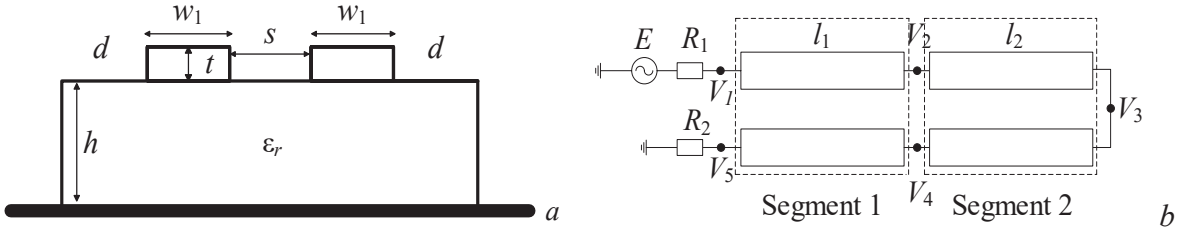

Figure 1. One segment cross-section view (*a*)
and the circuit diagram (*b*) of the line under investigation

Circuit diagram consists of two segments connected in cascade with a length of $l_{1,2}$=0.2 m, each of which consists of two parallel conductors. The first conductor of the first segment at the near-end is connected to a pulse signal source, represented by the e.m.f. source (E) with internal resistance R_1. The passive conductor of the first segment is connected to the receiving unit, represented by the resistance R_2. Resistances R_1 and R_2 are taken equal to 50 Ω. A trapezoidal pulse with the amplitude of the e.m.f. source is 1 V, the flat top, rise and fall times are 50 ps each is chosen as an excitation.

3. Expressions for calculating the amplitude of the signal at the line junctions

To plot lattice diagrams, we need to calculate the amplitude of the signal voltage at each point of the line under investigation. As the turn of a meander line is essentially a pair of coupled lines shorted at the far end, then according to modal analysis techniques, the incident wave voltage in the coupled line is a linear combination of modal voltages. This suggests that the processes involved in the propagation of each of the modes are isolated from each other, even at the terminations [15]. Then, a pair of coupled lines can be considered as two unconnected single lines. In one of the lines, an even mode propagates, and in the other an odd one. Before calculating the amplitudes of the transmitted and

reflected waves for each of the modes at each point of the line, we first introduce the matrix of modal voltages of the incident wave $\boldsymbol{U}_m$, the coefficients of which determine the amplitude of the incident wave of the even and odd modes at the beginning of the line

$$\boldsymbol{U}_m = \begin{bmatrix} U_m^e \\ U_m^o \end{bmatrix} = \boldsymbol{T}v^{-1}\boldsymbol{V} \tag{1}$$

where $\boldsymbol{T}_v$ is the matrix of eigenvectors of the product of Matrices **L** and **C** (conversion matrix), which for the pair of coupled lines with symmetrical cross-section has the view

$$\mathbf{T}v = \begin{bmatrix} Tv_{11} & Tv_{12} \\ Tv_{21} & Tv_{22} \end{bmatrix} = \begin{bmatrix} 0.707 & 0.707 \\ -0.707 & 0.707 \end{bmatrix}, \tag{2}$$

and the vector $\boldsymbol{V}$ upon excitation of one conductor of a pair of coupled lines has the view

$$\boldsymbol{V} = \begin{bmatrix} E \\ 0 \end{bmatrix} \tag{3}$$

where E is the e.m.f. source.

Then the amplitude of the incident wave of the even and odd modes at the junction between the source and the first line segment will be determined by the expressions

$$U_e = U_m^e \frac{Z_{e1}}{Z_{e1} + R_1} Tv_{11}, \;\; U_o = U_m^o \frac{Z_{o1}}{Z_{o1} + R_1} Tv_{12} \tag{4}$$

where $Z_{e,o1}$ is the impedance of the first segment for even and odd modes.

The amplitudes of the transmitted (U_T) and reflected (U_R) waves for the even and odd modes are determined by the expressions

$$U_{Te,o} = U_{e,o} T_{e,o}, \;\; U_{Re,o} = U_{e,o} \Gamma_{e,o} \tag{5}$$

where $\Gamma_{e,o}$ and $T_{e,o}$ are the transmission and reflection coefficients for even and odd modes at the junction, which for the junction between the source and the first segment will be calculated by the expressions from [13]

$$\Gamma_{Se} = \frac{R_1 - Z_{e1}}{R_1 + Z_{e1}}, \;\; \Gamma_{So} = \frac{R_1 - Z_{o1}}{R_1 + Z_{o1}}, \;\; T_{Se}=1+\Gamma_{Se}, \; T_{So}=1+\Gamma_S, \tag{6}$$

for the junction between the first and second segments, the coefficients will be calculated by the expressions

$$\Gamma_{e12} = -\Gamma_{e21} = \frac{Z_{e2} - Z_{e1}}{Z_{e2} + Z_{e1}}, \;\; \Gamma_{o12} = -\Gamma_{o21} = \frac{Z_{o2} - Z_{o1}}{Z_{o2} + Z_{o1}}, \tag{7}$$

$$T_{e12}=1+\Gamma_{e12}, \; T_{o12}=1+\Gamma_{o12}, \; T_{e21}=1+\Gamma_{e21}, \; T_{o21}=1+\Gamma_{o21}, \tag{8}$$

for the junction between the second segment and the received unit, the coefficients will be calculated by the expressions

$$\Gamma_{Le} = \frac{R_L - Z_{e2}}{R_L + Z_{e2}}, \;\; \Gamma_{Lo} = \frac{R_L - Z_{o2}}{R_L + Z_{o2}}, \;\; T_{Le}=1+\Gamma_{Le}, \; L_{Lo}=1+\Gamma_{Lo} \tag{9}$$

where $Z_{e,o2}$ is the impedance of the second segment for even and odd modes, R_L is the resistance at the far end. As we noted above, the junction between the conductors at the end of the turn (at the interconnection between half-turns) for the even mode is characterized by OC, and for the odd mode by SC. Therefore, expressions (9) after simple transformations as $R_L \to \infty$ for even and $R_L \to 0$ for odd modes take the view

$$\Gamma_{Le} = 1, \ \Gamma_{Lo} = -1, \ T_{Le} = 2, \ T_{Lo} = 0. \tag{10}$$

4. Analysis of lattice diagrams and time responses

To analyze the pulse signal propagation in a meander line of two segments, we plotted lattice diagrams (Figure 2) using expressions (5)–(10) for even and odd modes. On the left of the diagrams, the moments when pulses arrive at the line nodes are marked, and on the right, their amplitudes. To plot diagrams in the TALGAT software [16], we calculated the **C** and **L** matrices for the first and second segments

$$\mathbf{C}_1 = \begin{bmatrix} 169.35 & -39.54 \\ -39.54 & 169.35 \end{bmatrix} \text{ pF/m}, \ \mathbf{L}_1 = \begin{bmatrix} 431.85 & 157.28 \\ 157.28 & 431.85 \end{bmatrix} \text{ nH/m},$$

$$\mathbf{C}_2 = \begin{bmatrix} 126.96 & -35.25 \\ -35.25 & 126.96 \end{bmatrix} \text{ pF/m}, \ \mathbf{L}_1 = \begin{bmatrix} 549.74 & 215.15 \\ 215.15 & 549.74 \end{bmatrix} \text{ nH/m}.$$

Moreover, on the basis of the **C** and **L** matrices, we calculated impedances and per-unit-length delays of the even and odd modes of the first (Z_{e1}=67.36 Ω, Z_{o1}=36.25 Ω, τ_{e1}=8.74 ns/m, τ_{e2}=8.37 ns/m) and the second (Z_{e1}=91.35 Ω, Z_{o2}=45.37 Ω, τ_{o1}=7.57 ns/m, τ_{o2}=7.36 ns/m) segments.

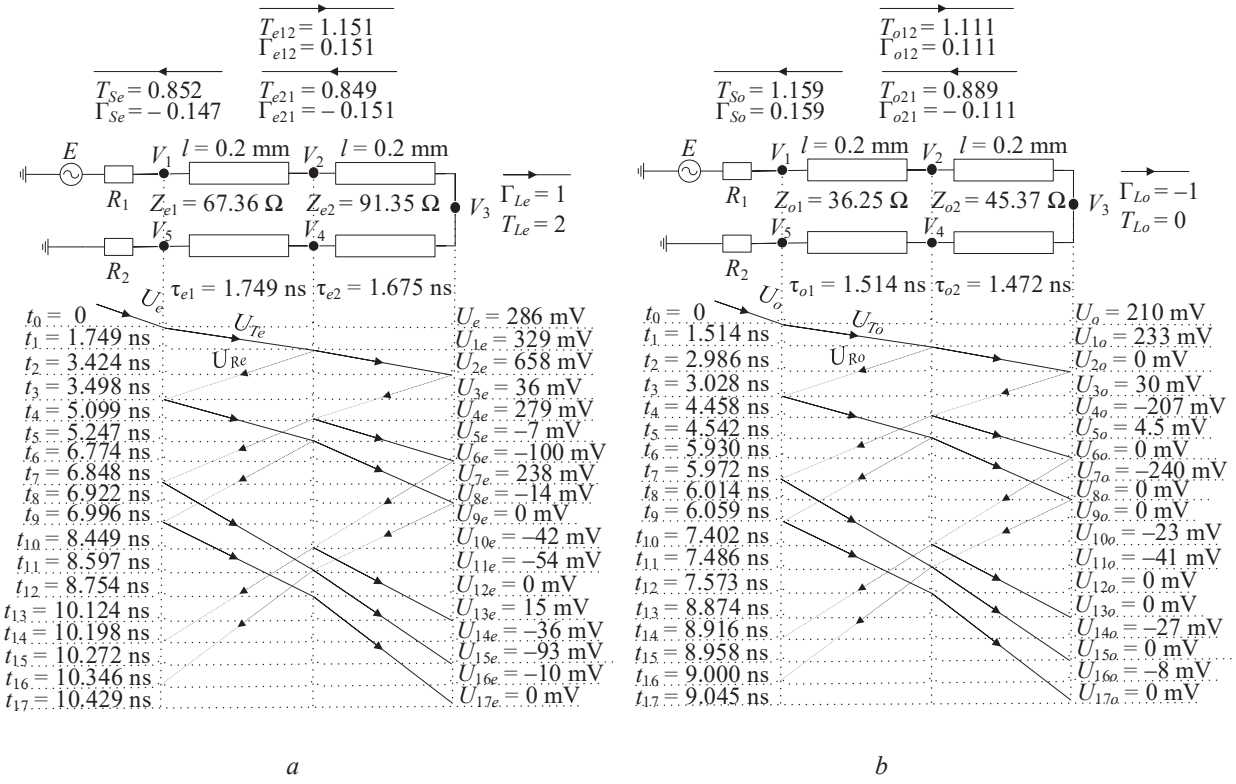

Figure 2. Lattice diagrams for even (*a*) and odd (*b*) modes

It can be seen from the diagram in Figure 2*a* that the first reflection of the transmitted wave arises from the junction between the segments with the reflection coefficient Γ_{e12}=0.151, and the reflected pulse arrives at node V_1 at time t_3 with a signal amplitude of 36 mV. Simultaneously, the transmitted pulse arrives at node V_3 with a delay t_2 and an amplitude of 658 mV because of the coefficient T_e=2, according to (10). The second reflected pulse arrives at node V_2 with a delay t_4 and an amplitude of 279 mV, because of the reflection coefficient Γ_e=1 from node V_3. Following the considered principle, it is possible to estimate the amplitude of the pulse signal at any node of the line, taking into account all reflections up to its complete attenuation. It can be seen from the diagram in Figure 2*b*, that the first reflection of the transmitted wave occurs from the junction between the first and second segments with a reflection coefficient Γ_{o12}=0.111. The reflected pulse arrives at node V_1 with a delay t_3 and an amplitude of 30 mV. The next reflection with the coefficient Γ_o=–1 in accordance with (10) arises from the junction between the half-turns (at node V_3). The pulse of the incident wave is completely reflected from this junction and arrives at node V_2 at time t_4 with an amplitude of –207 mV. Subsequent pulses are re-reflections from the junctions. Note that for an odd mode, in accordance with the coefficient T_o=0, similarly to the case of an SC in Figure 2*a* at times t_2, t_6, t_8, t_{13}, t_{15}, and t_{17}, the signal amplitude at node V_3 is 0. Finally, note that in Figure 2, pulses are observed whose amplitudes are close to 0 because they nearly completely attenuate as a result of reflections.

To assess the correctness of the obtained results in the TALGAT software, the voltage waveforms were calculated at all nodes of the line in Figure 1*b* for even and odd modes (Figure 3). For clarity and the possibility to compare them with diagrams (Figure 2), the voltage waveforms in all nodes of the circuit are summarized in one graph. The amplitudes of all pulses of the even and odd modes completely coincide with the amplitudes in the diagrams in Figure 2 calculated by expressions (5), as can be seen from the graphs.

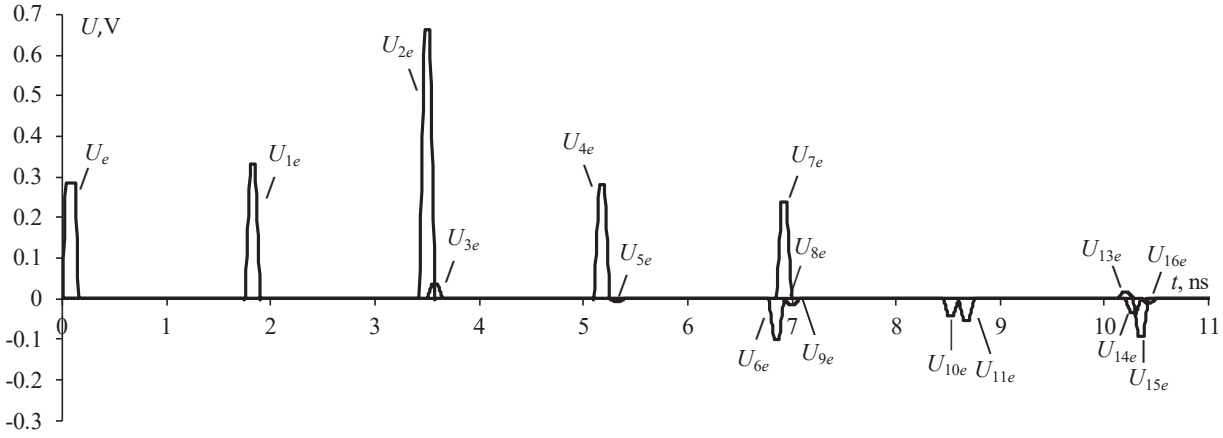

a

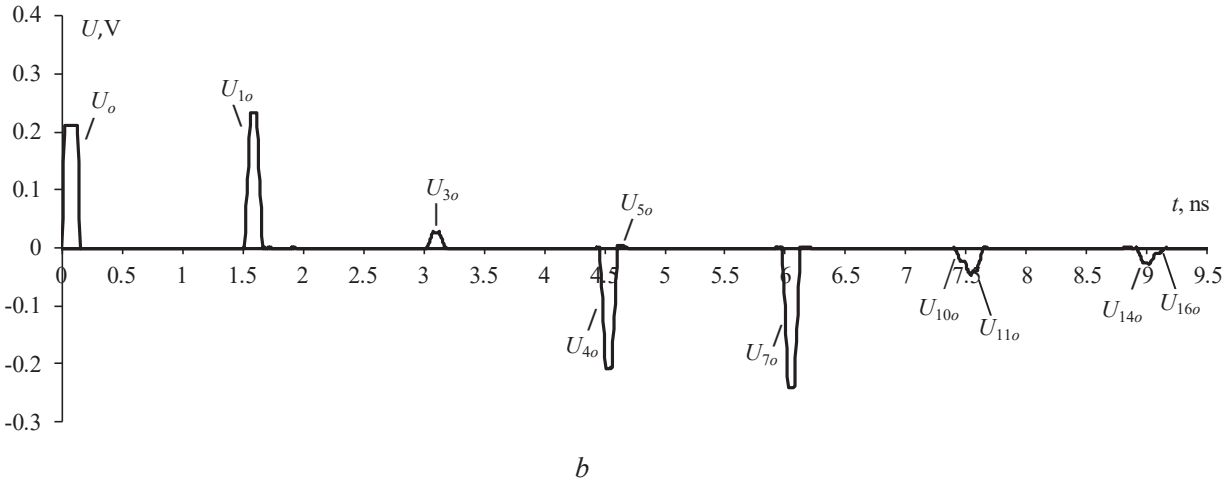

b

Figure 3. Voltage waveforms at the nodes of the circuit for even (*a*) and odd (*b*) modes

For the even mode, 15 pulses are observed in Figure 3*a*. The first three pulses are the main ones. Thus, the first pulse with an amplitude U_e=286 mV is an incident pulse, the second one with an amplitude U_{1e}=329 mV is a reflected pulse from the junction between the segments (node V_2) and propagating into the second segment, and the third one with an amplitude U_{2e}=658 mV is a reflected pulse from the junction between the second segment and the receiving unit (node V_3) and arriving at the end of the line. In addition to the main pulses, the graph contains pulses of different polarity, which are the result of reflections from the line junctions. For the odd mode, 10 pulses are observed in Figure 3*b* (due to). In Figure 3b, 10 pulses are observed for the odd mode. Only the first two pulses are basic (due to T_{Lo}=0). The first pulse is an incident wave pulse and has an amplitude U_o=210 mV, and the second is a transmitted wave pulse that arrives at node V_2 and has an amplitude U_{1o}=233 mV. All subsequent different polarity pulses are the result of multiple reflections from the junctions. Also, note that in Figure 3*b* at times t_2, t_6, t_8, t_{13}, and t_{15}, the signal amplitude at the V_3 node is 0, which is consistent with the diagram in Figure 2*b*. The amplitudes of the 9 and 12 pulses in Figure 3 are close to 0 because of attenuation resulting from reflections. Therefore, they are not plotted in the graphs.

5. Conclusion

The paper presents the analysis results for the pulse signal propagation in a turn of a meander line of two segments. Lattice diagrams for the even and odd line modes are plotted and then subsequently compared with the time responses at the line nodes. As a result, we revealed a complete coincidence of the amplitudes and arrival times of pulses obtained by different methods. In the future, it is advisable to study in detail the reflected pulses arising from the mismatch at the junctions of the segments as a resource for additional attenuation of USP amplitude.

Acknowledgments

The study was supported by the Russian Science Foundation grant 21-79-00161 in TUSUR.

References

[1] Fominich E N 2016 *Military Engineer* **2 (2)** pp 10–17
[2] Meshcheryakov S A 2013 *Journal of Radioelectronics* **12** pp 1–15
[3] Pirogov Yu A 2013 *Journal of Radioelectronics* **6** pp 1–3

[4] Gizatullin Z and Gizatullin R 2014 *Journal of Communications Technology and Electronics* **59 (5)** 463–466
[5] Gizatullin Z M and Gizatullin R M 2016 *Journal of Communications Technology and Electronics* **61 (5)** 546–550
[6] Messier M A, Smith K S, Radasky W A and Madrid M J 2003 *Proceedings of the 15th International Zurich symposium on EMC* pp 127–132
[7] Zdukhov L N, Parfenov L N, Tarasov O A and Chepelev V M 2018 *Journal of Technologies of electromagnetic compatibility* **2 (65)** 22–34
[8] Surovtsev R S, Nosov A V and Zabolotsky A M 2017 *IEEE Transactions on electromagnetic compatibility* pp 1864–1871
[9] Ramahi O M and Archambeault B 2001 *Proceedings of the International Zurich symposium on EMC* pp 537–539.
[10] Bhobe A U, Lolloway C, Piket-May M 2001 *International Symposium on EMC* pp 805–810
[11] Gazizov T R, Zabolotsky A M 2006 *Journal of Technologies of electromagnetic compatibility* 40–44
[12] Mikola P V and Surovtsev R S 2020 *International Scientific and Technical Conference Electronic Means and Control Systems (ESSU)* pp 304–306
[13] Hall S H and Hick H L 2009 *Advanced signal integrity for high-speed digital designs* (Published by John Wiley & Sons, Inc. Hoboken)
[14] Mikola P V, Kenzhegulova Z M and Surovtsev R S 2021 *International Scientific and Technical Conference Electronic Means and Control Systems (ESSU)* in press
[15] Park S W, Xiao F and Kami Y 2010 IEEE Transactions On Electromagnetic Compatibility **52** pp 436–446
[16] Kuksenko S P 2019 IOP Conference Series: Materials Science and Engineering (IOP Publishing) vol 560 p 012110